AIP | Applied Physics Letters

Surface area enhancement of microcantilevers by femto-second laser irradiation

A. Kumar, S. Rajauria, H. Huo, O. Ozsun, K. Rykaczewski, J. Kumar, and K. L. Ekinci

Citation: Applied Physics Letters **100**, 141607 (2012); doi: 10.1063/1.3701163
View online: http://dx.doi.org/10.1063/1.3701163
View Table of Contents: http://scitation.aip.org/content/aip/journal/apl/100/14?ver=pdfcov
Published by the AIP Publishing

Surface area enhancement of microcantilevers by femto-second laser irradiation

A. Kumar,[1] S. Rajauria,[2,3] H. Huo,[1] O. Ozsun,[4] K. Rykaczewski,[5] J. Kumar,[1] and K. L. Ekinci[4,a)]

[1]*Department of Physics and Center for Advanced Materials, University of Massachusetts Lowell, Lowell, Massachusetts 01854, USA*
[2]*Center for Nanoscale Science and Technology, NIST, Gaithersburg, Maryland 20899, USA*
[3]*Maryland Nanocenter, University of Maryland, College Park, Maryland 20742, USA*
[4]*Department of Mechanical Engineering and the Photonics Center, Boston University, Boston, Massachusetts 02215, USA*
[5]*Material Measurement Laboratory, NIST, Gaithersburg, Maryland 20899, USA*

(Received 12 March 2012; accepted 15 March 2012; published online 4 April 2012)

A dry single-step process for enhancing the surface area of a silicon microcantilever is described. In this process, a flat microcantilever is irradiated with ~100-femto-second-long laser pulses. The silicon surface melts and rapidly cools, resulting in the formation of nanoscale pillars. The shape and size of these nanostructures can be tuned by changing the energy of the pulses. Resonance measurements on surface-enhanced microcantilevers show that the irradiation process reduces the stiffness and the resonance frequency of the cantilevers. Fluidic dissipation measurements provide an estimate for the surface area increase. Both the enhanced surfaces and the fluidic characteristics of these microcantilevers may be useful in bio-chemical sensing applications. © *2012 American Institute of Physics*. [http://dx.doi.org/10.1063/1.3701163]

The microcantilever resonator is at the heart of numerous promising applications in micro and nanotechnology.[1] One such application is resonant bio-chemical sensing: here, one monitors the resonant oscillations of a microcantilever in order to detect small amounts of mass adsorbed on the microcantilever surface.[2–4] Shrinking the linear dimensions $l \times w \times t$ [Fig. 1(a) inset] of a microcantilever typically increases its mass sensitivity in resonant mass sensing.[1] This is because the cantilever effective mass M, which determines the mass sensitivity, is a linear function of the cantilever dimensions. However, as the cantilever dimensions are reduced, the surface area S of the cantilever goes down in addition to M. Since the capture of the analyte molecules is typically accomplished by a functional monolayer on the surface, the active sensing area of the cantilever sensor is reduced as a result of simple scaling.

To counter this, one must find ways to enhance the active sensing (surface) area of small devices. Various methods have been reported up to date.[5,6] However, these methods typically require multiple complicated micro-fabrication steps. Here, we report a single-step process to enhance the surface area of a microcantilever sensor. Our approach is based on irradiating the cantilever surface using a femto-second (fs) laser. It has been shown that exposure of silicon to fs pulses under the right conditions can generate structures on the surface with sub-micron linear dimensions.[7–9] To assess the effects of irradiation on the sensor properties, we investigate the change of the various parameters of the cantilever.

Our process is carried out using 400 nm light from a frequency-doubled amplified Ti:Sapphire laser. We use a 1 kHz train of 100 fs pulses with varying power to generate the surface modification. In this study, we have varied the average laser power from 60 mW to 100 mW (corresponding to a pulse energy of 60-100 μJ). The spatial profile of the laser pulses is nearly Gaussian with a beam waist of about 40 μm at the focal point. The irradiation of the cantilevers is done on a custom-made sample holder, which is filled with water. Thermal conduction through water prevents excessive temperature rise on the cantilevers during irradiation. The sample holder is mounted on a two-axis translation stage. The stage is rastered at a speed of 150 μm/s along the width w (y-axis) of the cantilever, and the separation between two consecutive scan lines along the length l (x-axis) is 100 μm. We typically place the cantilevers slightly out of focus

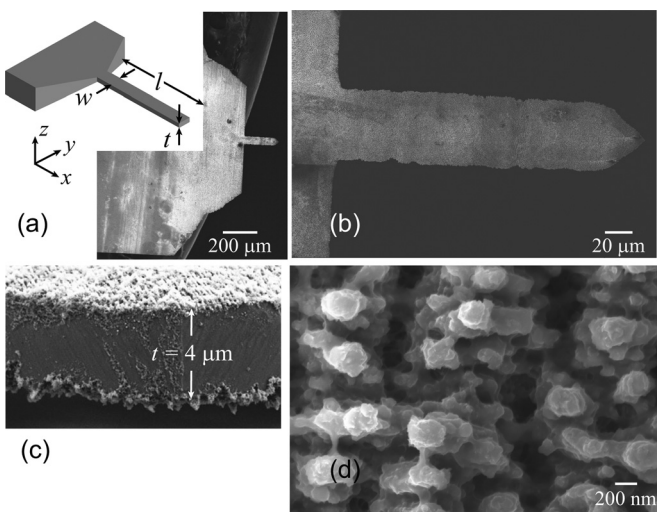

FIG. 1. (a) Scanning electron microscope (SEM) image of a cantilever chip after irradiation. The inset shows the dimensions and axes used in the text. (b) Top view image of a cantilever. (c) Tilt image showing the sidewall of a cantilever. (d) High magnification image of an irradiated cantilever showing submicron structure on the surface.

a)E-mail: ekinci@bu.edu.

(by ≈2 cm) during the irradiation to ensure overlap of adjacent irradiation passes.

Figures 1(a)–1(d) show examples of scanning electron microscope (SEM) images of irradiated microcantilevers at various magnifications and tilts. Figure 1(a) shows the entire chip, with the right-hand-side of the chip irradiated. Figures 1(b) and 1(c) show typical top view and side view images, respectively. Figure 1(d) is a close up top-view SEM image, showing sharp pillar-like structures on the surface of the cantilever. The pillars here are approximately 300 nm tall with widths around 200–300 nm and are separated from each other by $\sim 1\,\mu$m gaps. Some pillars appear to possess secondary nanostructures. Such features resulting from irradiation are reproducible and have been demonstrated on several cantilevers. Previous reports[7–9] suggest that these pillars are formed due to strong absorption of the fs laser pulses by the silicon surface and the subsequent fast cooling of the molten surface. Because direct measurement of this complex three dimensional surface topography on the cantilevers is challenging, we have inferred the degree of roughness indirectly from dissipation measurements.

We now turn to a detailed experimental study of the various mechanical and fluidic properties of the irradiated cantilevers. The parameters of the untreated and irradiated cantilevers are labeled with the subscripts 0 and 'i' respectively, in what follows. We first characterize the intrinsic mechanical properties of the surface-enhanced cantilevers. The fundamental mechanical resonances of all cantilevers are measured in vacuum and under ambient atmosphere both before and after irradiation. Here, the cantilevers are excited by a piezoelectric shaker and the ensuing motions are detected using a Michelson interferometer.[10] All resonance lineshapes obtained can be fitted by Lorentzians. Figure 2(a) is a typical measurement, which shows the fundamental resonance of a cantilever $(l \times w \times t = 125 \times 35 \times 4\,\mu\text{m}^3)$ in vacuum ($p \approx 10^{-2}$ Pa) and under atmospheric pressure before and after irradiation. The *in vacuo* quality factors are large throughout, $Q_v \sim 10^4$, and do not change appreciably with surface modification. The resonance frequency $\frac{\omega}{2\pi}$ shifts downward as a result of irradiation, as shown in Table I (compare columns labeled $\frac{\omega_0}{2\pi}$ and $\frac{\omega_i}{2\pi}$). The fluidic quality factor Q_f, which is found by properly subtracting Q_v from the atmospheric quality factor Q_{atm}, i.e., $Q_f^{-1} = Q_{atm}^{-1} - Q_v^{-1}$, also goes down. This effect is noticeable in columns labeled Q_{f0} and Q_{fi} in Table I.

The downward shift in the cantilever resonance frequency can be caused by a reduction in the stiffness K or an increase in mass M. Given that a mass increase during irradiation is rather improbable, K must go down. To provide support for this argument, we have measured K directly from the thermal-mechanical fluctuations, $\langle z^2 \rangle$, of the cantilever tip: $K \approx \frac{k_B T}{\langle z^2 \rangle}$, where $k_B T$ is the thermal energy. Figure 2(b) shows the thermal spectra of the same $125 \times 35 \times 4\,\mu\text{m}^3$ cantilever before and after irradiation with 75 mW/cm^2 power. These measurements are performed under ambient atmosphere. The noise spectral density can be integrated for both (before and after) curves to obtain $\langle z_0^2 \rangle = 26.5 \pm 3.8$ pm^2 and $\langle z_i^2 \rangle = 42.1 \pm 5.4$ pm^2, leading to $K_0 = 128 \pm 18$ N/m and $K_i = 80 \pm 10$ N/m, respectively (errors represent single standard deviations). As expected, the stiffness goes down due to irradiation.

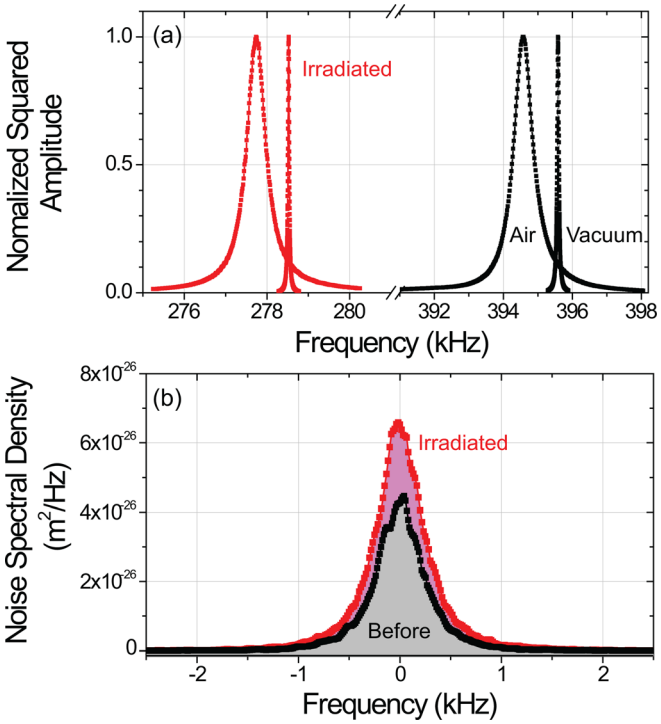

FIG. 2. (a) Fundamental flexural resonances of a cantilever before (black) and after (red) irradiation measured both in vacuum and in air. The linear dimensions ($l \times w \times t$) are $125 \times 35 \times 4\,\mu\text{m}^3$. (b) Thermal noise spectrum of the same cantilever. Resonance frequencies $\frac{\omega_0}{2\pi}$ and $\frac{\omega_i}{2\pi}$ have been subtracted from the frequency axis. The areas under the curves provide the stiffnesses K_0 and K_i.

Next, we turn to the decrease in fluidic quality factor Q_f (or the increase in fluidic dissipation $1/Q_f$) as a result of irradiation. Since the frequency is low, the surrounding air can be treated as a viscous fluid.[11] An approximation for Q_f can be found as[12]

$$Q_f = \frac{\frac{4\rho_{Si} t}{\pi \rho_{air} w} + \Gamma'(\omega)}{\Gamma''(\omega)}. \tag{1}$$

Here, $\Gamma'(\omega)$ and $\Gamma''(\omega)$ are the real and imaginary components of the complex hydrodynamic function, and ρ_{Si} and ρ_{air} are the respective densities of Silicon and air. In order to see any irradiation effects, one must compare the fluidic dissipation between cantilevers of the same size and deconvolute any trends arising from the difference in resonance frequencies. In a gaseous medium, the virtual fluid mass is small and its contribution to dissipation can be neglected, resulting in $Q_f \approx \frac{4\rho_{Si} t}{\pi \rho_{air} w} \times \frac{1}{\Gamma''}$. The dimensionless quantity,

TABLE I. Parameters of different microcantilevers irradiated at different power levels. The parameters of the irradiated cantilevers are labeled with the subscript 'i' while the parameters of the untreated cantilevers are labeled with 0.

$l \times w \times t$ (μm^3)	P (mW)	$\frac{\omega_0}{2\pi}$ (kHz)	Q_{f0}	$\frac{\omega_i}{2\pi}$ (kHz)	Q_{fi}
$225 \times 40 \times 8$	60	202	763	191	682
$125 \times 35 \times 4$	75	395	648	278	535
$225 \times 40 \times 8$	80	202	743	173	645
$225 \times 40 \times 8$	100	202	720	155	507

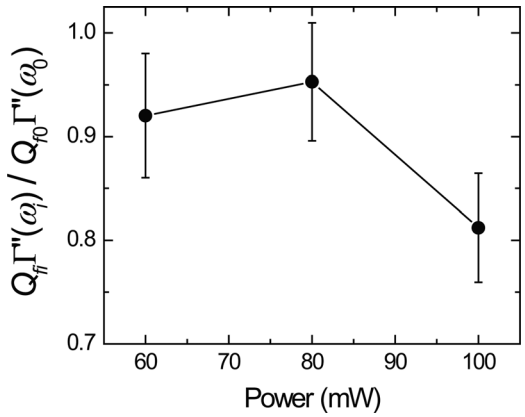

FIG. 3. Fluidic dissipation of the cantilevers as a function of the irradiation power. The data are presented as a ratio of the fluidic quality factors Q_f measured before and after irradiation. The effects of the frequency differences are de-convoluted by multiplying the Q_f with the imaginary component $\Gamma''(\omega)$ of the complex hydrodynamic function. Error bars show the associated single standard deviations.

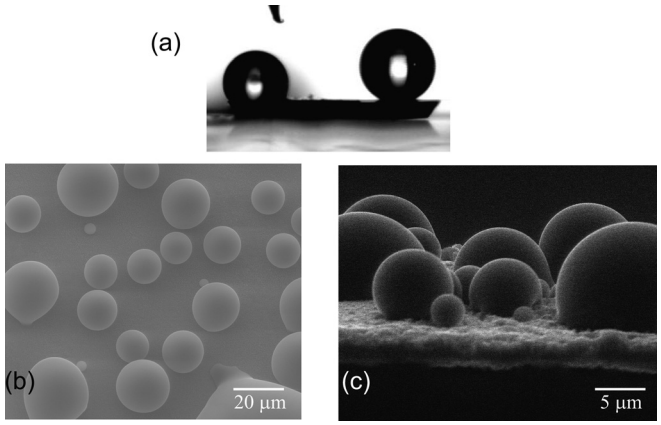

FIG. 4. (a) Contact profiles of water droplets on the chip after silanization. The right side of the chip has been irradiated. (b) ESEM images of the chip with condensed water micro-droplets. (c) ESEM image of microdroplets on the microcantilever.

$Q_f\Gamma''(\omega) \approx \frac{4\rho_{Si}t}{\pi\rho_{air}w}$, depends only on the linear dimensions w and t of the cantilever. We can, therefore, elucidate the effects of irradiation on the surface by forming the ratio, $\frac{Q_{fi}\Gamma''(\omega_i)}{Q_{f0}\Gamma''(\omega_0)} \approx \frac{t_i}{t_0} \times \frac{w_0}{w_i}$. Figure 3 (main) shows $\frac{Q_{fi}\Gamma''(\omega_i)}{Q_{f0}\Gamma''(\omega_0)}$ for cantilevers with the same linear dimensions of $l \times w \times t = 225 \times 40 \times 8\ \mu\text{m}^3$. The fact that $\frac{Q_{fi}\Gamma''(\omega_i)}{Q_{f0}\Gamma''(\omega_0)} < 1$ for all irradiated cantilevers suggests that the *effective* surface area[13] of the cantilevers increases as a result of irradiation. It is clear that the *average* macroscopic linear dimensions of the cantilevers do not change upon irradiation; the result suggests a microscopically rougher surface, $S_i > S_0$, where $S_0 \approx 2wl$

The surface enhancement described here has a variety of potential applications. One such application is in anti-wetting or low adhesion coatings for MEMS and NEMS. To demonstrate this, we have vapor-coated the surface enhanced cantilever by fluorinated-silane (1H, 1H, 2H, 2H-perfluorooctyl trichlorosilane). Figure 4(a) shows two water droplets placed on the cantilever chip, one on the region roughened by irradiation and the other on the flat chip surface. Clearly, the irradiation makes the chip surface superhydrophobic with contact angle around 155°. To see whether or not the cantilever surface also becomes superhydrophobic, we have further imaged the samples in an environmental scanning electron microscope (ESEM). Water condensation is induced on the chip by increasing the water vapor pressure in the ESEM chamber from 600 Pa to 700 Pa while holding the temperature of the sample constant at 0 °C. Figure 4(b) shows the condensation of water droplets on the rough areas of the silanized chip. Figure 4(c) shows the condensation on the cantilever surface. While the contact angle varies between micro-droplets, the cantilever surface appears superhydrophobic. The average contact angle on silane coated rough cantilever surfaces is found to be ~115°. The variation in the contact angle, apparent in Fig. 4(c), is due to electron beam degradation of the silane coating.[14]

In conclusion, we have developed a dry single-step process to enhance the surface area of microcantilevers. The process could be applied to MEMS and NEMS based sensors. This process can also be useful in fundamental studies, such as correlating the effect of nanoscale roughness to energy dissipation in mechanical resonators under a variety of conditions.

The authors acknowledge support from the US NSF (through Grant Nos. ECCS-0643178, CBET-0755927, CMMI-0970071, and 52100000005103). K.R. was supported by an NRC ARRA postdoctoral fellowship at NIST.

[1]K. L. Ekinci and M. L. Roukes, Rev. Sci. Instrum. **76**, 061101 (2005).
[2]K. L. Ekinci, X. M. H. Huang, and M. L. Roukes, Appl. Phys. Lett. **84**, 4469 (2004).
[3]B. Ilic, Y. Yang, K. Aubin, R. Reichenbach, S. Krylov, and H. G. Craighead, Nano lett. **5**, 925–929 (2005).
[4]L. A. Pinnaduwage, V. Boiadjiev, J. E. Hawk, and T. Thundat, Appl. Phys. Lett. **83**, 1471 (2003).
[5]R. E. Fernandez, S. Stolyarova, A. Chadha, E. Bhattacharya, and Y. Nemirovsky, IEEE Sens. J. **9**, 1660 (2009).
[6]S. H. Bhansali, J. M. Jarvis, I. A. Aksay, and J. D. Carbeck, Langmuir **22**, 6676–6682 (2006).
[7]C. Momma, S. Nolte, B. N. Chichkov, F. v. Alvensleben, and A. Tunnermann, Appl. Surf. Sci. **109/110**, 15 (1997).
[8]E. N. Glezer, M. Milosavljevic, L. Huang, R. J. Finlay, T.-H. Her, J. P. Callan, and E. Mazur, Opt. Lett. **21**, 2023 (1996).
[9]T. -H. Her, R. J. Finlay, C. Wu, S. Deliwala, and E. Mazur, Appl. Phys. Lett. **73**, 1673 (1998).
[10]A. Sampathkumar, T. W. Murray, and K. L. Ekinci, Appl. Phys. Lett. **88**, 223104 (2006).
[11]K. L. Ekinci, V. Yakhot, S. Rajauria, C. Colosqui, and D. M. Karabacak, Lab Chip **10**, 3013–3025 (2010).
[12]J. E. Sader, J. W. M. Chon, and P. Mulvaney, Rev. Sci. Instrum. **70**, 3967 (1999).
[13]G. Palasantzas, J. Appl. Phys. **104**, 016107 (2008).
[14]K. Rykaczewski, J. Chinn, M. L. Walker, J. H. J. Scott, A. Chinn, and W. Jones, ACS Nano **5**, 9746 (2011).